DOI: 10.1002/ejic.200700784

Flexible Cu^{I}–Thiolate Clusters with Relevance to Metallothioneins

Biplab K. Maiti,[a] Kuntal Pal,[a] and Sabyasachi Sarkar*[a]

Keywords: Metallothioneins / Flexibility / Coordination modes / Copper / Sulfur / Photoluminescence

Simple Cu–thiolate chemistry was developed to demonstrate the presence of copper clusters with $\{Cu_4S_6\}$, $\{Cu_5S_7\}$ and $\{Cu_6S_4\}$ cores in relevance to copper-containing metallothioneins. The new hexanuclear tricoordinate triply bridging thiolatocopper(I) clusters $[NEt_4]_4[Cu_6(SPh)_4Cl_6]$ (**1**) and $[NEt_4]_4[Cu_6(SPh)_4Br_6]$ (**2**) were synthesized from the soup of polymeric $[Cu^{I}SPh]_n$ and quaternary ammonium halide. These complexes readily converted into $[Et_4N]_2[Cu_5(SPh)_7]$ (**3**) and $[Et_4N]_2[Cu_4(SPh)_6]$ (**4**) in the presence of excess amounts of thiol. All are structurally characterized by single-crystal X-ray crystallography and these smaller clusters may be inscribed into the structurally characterized larger cluster $\{Cu_8S_{10}\}$ obtained from synthetic copper yeast metallothioneins. Like Cu–MT proteins, all these clusters show photoluminescence around 560 nm on excitation at 350 nm, and these emission spectra are completely quenched by molecular oxygen. Variable copper stoichiometry and the interconversion of only monodentate thiolate ligands in these clusters convey the importance of flexibility, which is relevant to metallothioneins.

Introduction

Intracellular copper is transiently associated with small copper-binding proteins as copper chaperones that distribute copper to specific intracellular destinations and to metallothioneins (MT). MT is a class of low molecular weight cysteine rich proteins that generally shuffle essential metal ions like copper and zinc in biosystems, and they are present in all animal phyla as well as in certain fungi, plants and cyanobacteria.[1–7] The protection of cells against toxic metal ions through the process of sequestration is another role played by these proteins. MT proteins from varied species showed to share a particular set of sequence-specific characters with the consensus sequence -CxCxxxxCxC- and -CxCxxxxxCxC- motifs.[8] These four cysteine units may thus be used to complex copper ions besides other cysteine moieties located differently in apo-MT proteins. In Cu–MT coordination chemistry, the Cu^{I}/protein stoichiometry is varied because of the diverse functions of copper, such as acquisition, metabolism, storage and transport. Among these, in vitro synthesized N.crassa MT was shown to provide flexible polypeptide folds that may be influenced by the variable coordination number of copper, which results from metal–thiolate clusters with varied stoichiometries, such as $Cu_4(CysS)_7$(Cu_4–NcMT) or $Cu_6(CysS)_7$(Cu_6–NcMT).[8] A neuronal growth inhibitory factor, metallothionein-3, was shown to contain the $Cu_4(CysS)_9$ (Cu_4-humanMT-3) cluster located in the N-terminal β-domain of the protein, which can further be loaded with copper to yield a $Cu_6(CysS)_9$ cluster.[9] The isolation of a synthesized $Cu_8(CysS)_{10}$(Cu_8-yeastMT) cluster is thought to crystallize from a solution of Cu_7-yeastMT, which leaves the Cu_6 cluster in solution.[10] In contrast to zinc, which normally retains a tetrahedral coordination, the ready adaptation of Cu^{I} to diagonal, trigonal or tetrahedral coordination geometries has made the chemistry of Cu–MT diverse and interesting. In the large Cu_8–S_{10} cluster, the only two diagonal Cu binding sites are thought to be responsible for trafficking copper in biological systems, and this ability is attributable to the labile bonding of these two copper atoms.[10,11] Prediction of the formulation of the copper–thiolate cluster is also hindered by the ability of the sulfur atom of the cysteinyl moiety to link the bridging ligand in a μ_2-S or μ_3-S fashion. Furthermore, the possibility of a large degree of folding in the protein may account for the structural interplay of these copper clusters. Among the common Cu_n clusters (n = 4,[12] 6,[8,9] 7[13] and 8[10,11]) known to be present in Cu–MT, the varied ligation number of the thiolate ion ($CysS_m$, m = 4 to 11) contributes to the diverse stoichiometry that one can anticipate in Cu–MT clusters. Accordingly, many examples of monodentate thiolatocopper(I) clusters have been reported so far by X-ray crystallography[14–16] [CuS_2,[17] CuS_3,[18,19] Cu_2S_2,[20] Cu_3S_3,[21] Cu_4S_4,[22] Cu_4S_6,[18,23–26] Cu_5S_6,[27,28] Cu_5S_7,[29] Cu_6S_4 (in this work) Cu_7S_8,[30] Cu_8S_8[31] and $Cu_{12}S_{12}$[32]].

[a] Department of Chemistry, Indian Institute of Technology Kanpur,
Kanpur 208016, India
Fax: +91-512-2597265
E-mail: abya@iitk.ac.in
Supporting information for this article is available on the WWW under http://www.eurjic.org or from the author.

On the basis of this principle, we allowed the free assembly of discrete copper(I)–thiolate clusters from the soup of polymeric $[Cu^ISPh]_n$[33] and quaternary ammonium halide in the presence or absence of an excess amount of thiolate ions. We report herein the first synthesis of the hexanuclear tricoordinate triply bridging thiolatocopper(I) clusters $[NEt_4]_4[Cu_6(SPh)_4Cl_6]$ (**1**) and $[NEt_4]_4[Cu_6(SPh)_4Br_6]$ (**2**). They were characterized by X-ray crystallography as well as by spectroscopic methods, including UV/Vis and luminescence, and their ready interconversion with $[Et_4N]_2[Cu_5(SPh)_7]$ (**3**) and $[Et_4N]_2[Cu_4(SPh)_6]$ (**4**). All these smaller clusters may be inscribed into the structurally characterized larger cluster $\{Cu_8S_{10}\}$ obtained from the synthesized copper yeast metallothioneins. From a synthetic analogue approach, the present study is based on the filling of this gap to achieve this specific cluster arrangement.

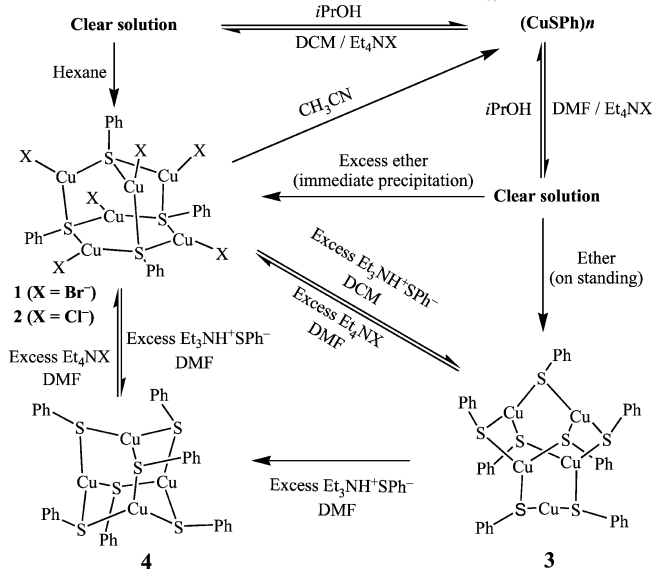

Scheme 1. The facile interconversion of Cu_4-, Cu_5- and Cu_6 clusters.

Results and Discussion

Synthesis

Cu^I–thiolate clusters are known and earlier synthetic strategies generally involved the use of Cu^{II} ions to exploit the reducing power of the thiolate group used as a ligand. This synthetic protocol led to the formation of a mixture of products such as $[Me_4N]_2$ salt of **3** and **4**[34] and both were crystallized out. In another procedure, the use of Cu^I as the source material was made and this was treated with KSPh in acetonitrile and the $[PPh_4]_2$ salt of **4**[18] was isolated. Alternatively, $[PPh_4]_2[Cu(SPh)_3]$[18] was treated with $[Cu(CH_3CN)_4]ClO_4{\cdot}2H_2O$ in boiling acetonitrile to synthesize the same compound, but the yield of the product in these procedures was not reported. In the present work, our intention was to understand the solubility of the Cu–thiolate polymer in the form of isolable discrete cluster anions as quaternary ammonium ion salts in the presence or absence of an excess amount of thiolate ions. The hexanuclear copper(I)–thiolate complexes having $Cu_6S_4X_6$ (X = Cl^- and Br^-) (Scheme 1) were synthesized by treating $(CuSPh)_n$[33] with the respective quaternary ammonium halide salt (Et_4NX) in a 1:1 molar ratio of CuSPh/Et_4NX to produce **1** and **2** as block-shaped colourless crystals in high yield.

By changing the reaction medium and by performing the reaction in the presence of available thiolate ions, the synthesis of **3** and **4** and the mutual interconversion of all four (**1**–**4**) of these discrete clusters was followed by electronic spectroscopy as shown in Figure S1 (Supporting Information). Our attempt to increase the ligation of the thiolate ions by metathesis of **1** or **2** by anticipating the formation of $\{Cu_6(SPh)_{10}\}$ in light of attaining maximum thiolate ligation similar to those reported in the MT proteins was thwarted by the isolation of **3** and **4** instead. Compound **3** was synthesized by the reaction of CuSPh with Et_4NCl in a 1:1 molar ratio in DMF as bright-yellow needle-shaped crystals in high yield. It is noteworthy that **3** crystallized out of solution on standing after the addition of diethyl ether. In contrast, the addition of an excess amount of diethyl ether caused rapid precipitation of the Cu_6 cluster instead. The reactions of **1** or **2** with excess amounts of thiolate ions afforded solvent-dependent formation of **3** and **4** in almost quantitative yields. In less polar solvents, such as DCM, the reaction of **1** or **2** with an excess amount of thiolate afforded **3**, whereas in more polar solvents, such as DMF, the reaction led to the formation of **4**. It was found that the transformation of **1** into **3** was very facile in the reverse direction. The reversal of **4** to **1** or **2** may also readily be achieved by the addition of an excess amount of countercation in DMF, but **3** may be converted irreversibly into **4** in DMF. Compounds **1** and **2** in CH_3CN, and in any other protic solvent, decompose with the precipitation of insoluble $(CuSPh)_n$[33] and the release of $[Et_4N]X$ (X = Cl and Br) into the solution. The interconversion between these compounds is dependent on the solvent used and on the Cu/S ratio. The Cu/S ratio in Cu–MT may be affected by the surrounding environment or even by a variation in the cysteine content of the peptide; however, it is important to note that the availability of Cu is the key factor affecting the stoichiometry of the Cu/S clusters in MT. All these compounds, when present in solution, are susceptible to aerial oxidation, which leads to decomposition. Even in the solid state, surface oxidation of **1** or **2** is noticed on exposure to air, and the surface turns from pure white to white with a greenish tinge. EPR response of this reaction clearly indicates that EPR inactive Cu^I is oxidized to EPR active Cu^{II}.

Description of Structures

Suitable diffraction quality single crystals of all the reported complexes were made according to the procedure described in the corresponding synthesis section. Details of the crystallographic data collection and refinement parameters are provided in Table 3.

Crystals of chloro and bromo compounds **1** and **2**, respectively, are isostructural, triclinic, $P\bar{1}$ and have the same number of formula units ($Z = 2$) in each unit cell of very similar dimensions. Complexes **1** and **2** exhibit a $Cu_6S_4X_6$ core (Figure 1), which is constructed from the aggregation of six Cu^I centres, six halide (Cl or Br) atoms and four S (benzenethiolate) atoms.

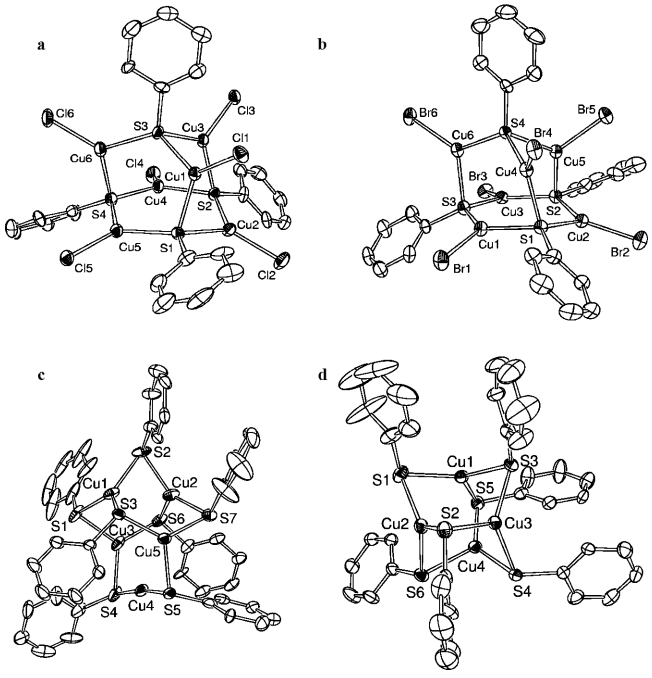

Figure 1. The structure (ORTEP view) of the complex anion of (a) **1**; (b) **2**; (c) **3** and (d) **4**. The atomic numbering scheme is shown and the thermal ellipsoids are drawn at the 50% probability level; hydrogen atoms have been omitted for clarity.

Compounds **1** or **2** can be divided into two segments to form one $Cu_3S_3X_3$ unit (bottom segment) and one Cu_3SX_3 unit (top segment) (atoms labelled with superscript b and t, respectively). These two units are bound by the S atom of the thiolate that bridges two Cu atoms in $Cu^b{}_3S^b{}_3$ and is bound to the Cu atom in $Cu^t{}_3S^t$. The top S^tPh ligand is directed axially and is perpendicular to the virtual $Cu^t{}_3$ plane. Each copper atom in the top is three coordinate and forms bonds from one S atom and one halogen atom in the same segment and one S atom from the bottom segment. In this way, a core is formed that comprises a fused six-membered Cu_3S_3 ring: one for the bottom (almost planar hexagon) and three for the side faces (pseudochair configuration). Each copper atom in the bottom is three coordinate with bonds from two S atoms and one halogen atom in the same segment, and these S^bPh ligands are around the equatorial girdle and form a virtual $Cu^b{}_3$ plane. The two Cu_3 triangle bases are oriented face-to-face and are rotated by ca. 45°. Each copper centre in the cluster adopts an approximately trigonal planar geometry, and it is coordinated to two thiolate ligands and a halide ion. The mean angle at the coordinated copper is 119.75(7)° for **1** and 119.95(6)° for **2**, which suggests an almost trigonal planar geometry of the copper centre in these complexes. Each sulfur atom of the phenylthiolate ligand within the cluster adopts an approximate tetrahedral geometry that coordinates three trigonally coordinated copper atoms (triply bridging thiolate ligand). The Cu–S bond lengths [mean 2.2465(17) Å for **1** and mean 2.2502(18) Å for **2**][35] are dependent on the coordination number of the copper atom and distinct ranges can be distinguished: 2.14–2.17 Å for two coordinate[29,36] copper atoms, 2.22–2.23 Å for three coordinate[18,23–26,37] copper atoms and 2.33–2.48 Å for four coordinate[38–40] copper atoms, and the Cu···Cu separations range from 2.8622(12) to 4.0699(13) Å for **1** and from 2.8242(13) to 4.0557(13) Å for **2**. Bond lengths and angles are listed in Table 1.

The type of Cu_4S_6 and Cu_5S_7 core[18,23,26,29] observed for **3** and **4** (Figure 1), respectively, were structurally characterized previously for monodentate S donor ligands in $[Cu_4(SPh)_6]^{2-}$ and $[Cu_5(SPh)_7]^{2-}$ with $[Me_4N]$ and $[PPh_4]$ salts, and the dimension of these cores as $[Et_4N]$ salts are detailed in Table 3. Complexes **1**, **2** and **4** possess tricoordinated copper; in **1** and **2** μ_3-SPh bridging exists, whereas in **4**, μ_2-SPh bridging is present. Unlike **1**, **2** or **4**, compound **3** possesses both tri- and bicoordinated copper but with only a μ_2-SPh bridging ligand. Similar to **1** or **2**, the Cu–S bonds in Cu–thiolate bridges in **3** or **4** range from 2.159 to 2.309 Å. This may be compared with the Cu–S–Cys bonds in the range from 2.145 to 2.395 Å found in the structurally characterized $Cu_8(CysS)_{10}$ (Cu_8-yeastMT) cluster.[10] The $Cu_8(CysS)_{10}$ (Cu_8-yeastMT) cluster[10] can be described as two groupings of four copper atoms; both groups have a flattened tetrahedron structure and two of the eight copper atoms are diagonally coordinated and the six others are trigonally coordinated with doubly and triply bridging cysteine moieties, as highlighted in Figure 2.

Structurally characterized clusters **1**, **2**, **3** and **4** may be inscribed within the structurally characterized $Cu_8(CysS)_{10}$ (Cu_8-yeastMT) cluster in Figure 2 and comparison of the Cu–S distance in **1**, **2**, **3**, **4** and $Cu_8(CysS)_{10}$ (Cu_8-yeastMT) cluster are listed in Table 2. In Figure 2, cluster **4** is placed on the left side (Cu1, Cu2, Cu3 and Cu4) of the larger cluster, $Cu_8(CysS)_{10}$ and **3** are placed on the right side (Cu4, Cu5, Cu6, Cu7 and Cu8) of the larger cluster $Cu_8(CysS)_{10}$, and both share one common copper atom (Cu4). The Cu1 atom of the larger cluster is bonded with S1 and S3 but Cu1 in **4** is tricoordinated with an extra bond to S5. The bicoordinated Cu1 in Cu_8-yeastMT is directly related to its labile nature in displaying copper trafficking properties. The two diagonally coordinated copper ions (Cu1 and Cu8) are more labile than other copper atoms in $Cu_8(CysS)_{10}$. In this respect, Cu_6 clusters **1** or **2** are more important. In Figure 2, the six copper ions in $Cu_8(CysS)_{10}$ [(Cu2, Cu4 and Cu6) and (Cu3, Cu7 and a missing Cu as shown encircled)] can be described as grouped into two set of three, both of which have planar triangle geometry and linked by sulfur. A closer inspection shows that for Cu_8-yeastMT, middle part of the skeleton have similar structural motif of **1** or **2** as shown in Figure 2.

Table 1. Bond lengths (Å) and angles (°) of **1** and **2**.

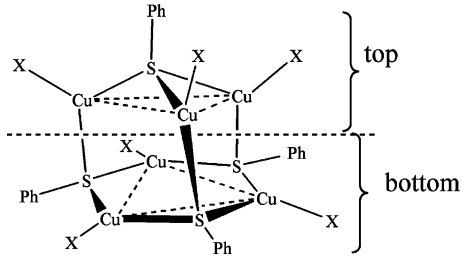

X = Cl (1) and Br (2)

Parameter	Range (average) of **1**	Range (average) of **2**
Within top segment[a]		
Cu–S	2.244–2.258 (2.251)	2.243–2.251 (2.245)
Cu···Cu	2.862–3.860 (3.504)	2.833–3.819 (3.484)
Cu–S–Cu	79–118 (105)	78–117 (103)
Cu–Cu–Cu	44–69 (60)	44–69 (60)
Within bottom segment[a]		
Cu–S	2.244–2.258 (2.251)	2.243–2.251 (2.245)
Cu···Cu	2.862–3.860 (3.504)	2.833–3.819 (3.484)
Cu–S–Cu	79–118 (105)	78–117 (103)
Cu–Cu–Cu	44–69 (60)	44–69 (60)
Interaction from top to bottom[a]		
Cu–S	2.236–2.268 (2.250)	2.230–2.265 (2.247)
S–Cu–S	103–118 (113)	105–122 (115)

[a] See above schematic representation.

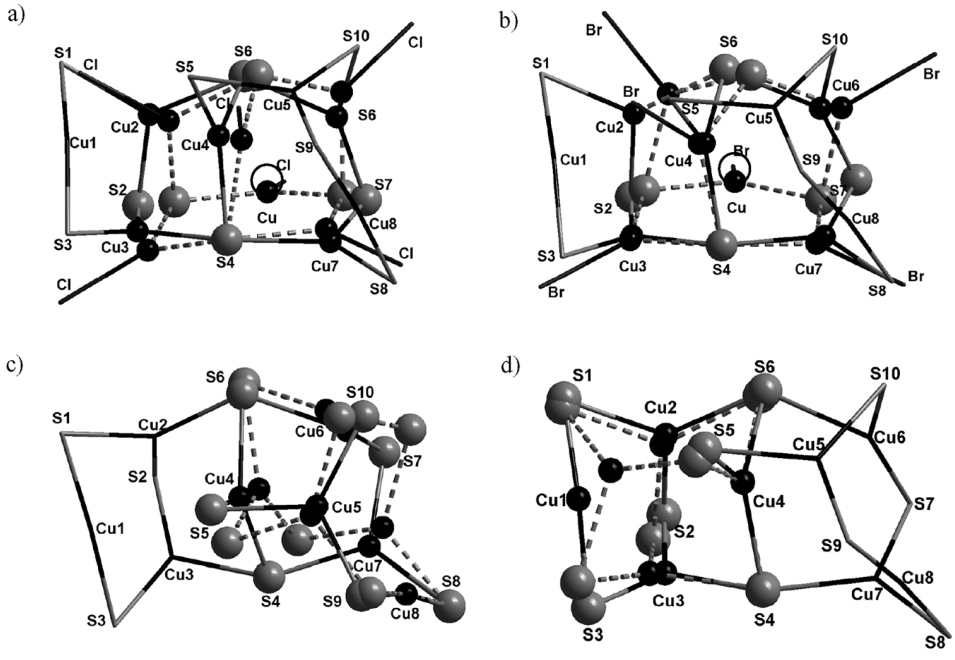

Figure 2. Ball & stick models: (a) superposition of the $\{Cu_6S_4\}$ framework (broken line) of complex anion **2** and the $\{Cu_6S_4\}$ core (represented Cu2–S2–Cu3–S4–Cu4–S6–Cu6–S7–Cu7 and one missing copper position marked in circle) of Cu_8-yeastMT; (b) superposition of the $\{Cu_6S_4\}$ framework (broken line) of complex anion **1** and the $\{Cu_6S_4\}$ core (represented Cu2–S2–Cu3–S4–Cu4–S6–Cu6–S7–Cu7 and one missing copper position marked in circle) of Cu_8-yeastMT; (c) superposition of the $\{Cu_5S_7\}$ framework (broken line) of complex anion **3** and the $\{Cu_5S_7\}$ core (represented Cu4–S4–S5–Cu5–S9–S10–Cu6–S6–Cu7–S7–Cu8–S8) of Cu_8-yeastMT; (d) superposition of the $\{Cu_4S_6\}$ framework (broken line) of complex anion **4** and the $\{Cu_4S_6\}$ core (represented Cu1–S1–Cu2–S2–Cu3–S3–S4–Cu4–S5–S6) of Cu_8-yeastMT.

Table 2. Comparison of Cu–S distances in **1**, **2**, **3**, **4** and Cu_8–MT.

Parameter	**1**	**2**	**3**	**4**	Cu_8–MT
Bridging mode of S	μ_3-SR	μ_3-SR	μ_2- & μ_3-SR	μ_2-SR	μ_2- & μ_3-SR
Coordination at Cu centre	S_2Cl	S_2Br	S_2 & S_3	S_3	S_2 & S_3
Cu–S	2.244–2.258 Å	2.243–2.251 Å	2.160– 2.297 Å	2.245–2.306 Å	2.139–2.395 Å

Electronic and Photoluminescent Spectra

Complexes **1** and **2** are colourless and display featureless electronic spectra with a strong absorption in the UV region. As shown in Figure 3, the UV/Vis absorption spectrum of **1** in DCM showed a strong absorption centred at λ_{max} = 272 nm (ε = 27800 $M^{-1}cm^{-1}$). Likewise, the absorption spectrum for complex **2** is similar: λ_{max} = 266 nm (ε = 33100 $M^{-1}cm^{-1}$).

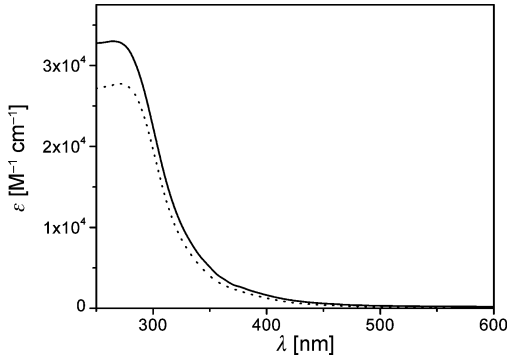

Figure 3. Absorption spectra of complex **1** (broken line) and **2** (solid line) at room temperature in DCM.

Excitation spectra of solid samples of hexanuclear copper(I) complexes **1** and **2** are shown in Figure 4. Compound **2** exhibits a broad excitation band centred at λ_{ex} = 346 nm with a weak shoulder at 425 nm, whereas an intense band is observed at λ_{ex} = 346 nm for corresponding solid complex **1**.

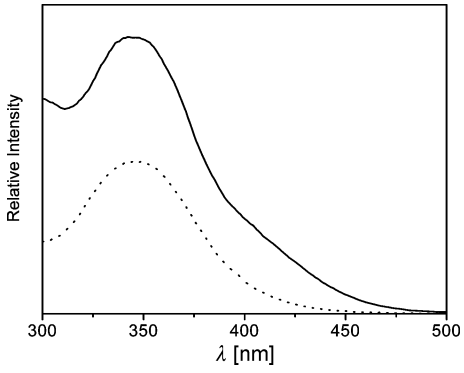

Figure 4. Excitation spectra of **1** (broken line) and **2** (solid line) at room temperature in the solid state.

Photoluminescence is a powerful tool to investigate the structural information of Cu–MTs because of the characteristic luminescence properties of the Cu^I–thiolate clusters. Complexes **1** to **4** display photoluminescence like other copper–sulfur clusters.[41,42] Compounds **1**, **2** and **3** each exhibit an intense emission band in the range 555–573 nm (excitation at 350 nm), whereas under identical conditions, a very weak emission at 572 nm (excitation at 350 nm) was observed from **4** (Figure 5). Possible assignment of transition is considered as: (1) ligand-to-metal CT (LMCT), (2) the halide-to-metal CT (XMCT), (3) transition in Cu cluster (CC–MOs), (4) halide-to-ligand CT (XLCT) and (5) Cu^I d–s transition.

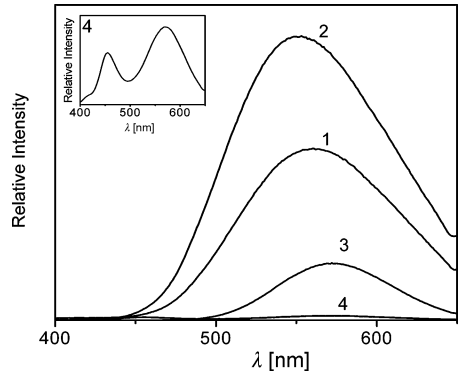

Figure 5. Emission spectra of **1** (560 nm), **2** (555 nm), **3** (573 nm) and **4** (572 nm) at room temperature in the solid state (excitation at 350 nm); inset: the emission spectra of **4** in relatively enlarged scale of intensity.

From a structural viewpoint, cluster **1** and **2** (Cu_6 cluster) both have long Cu···Cu separations (>2.8 Å). So, transition in Cu clusters (CC–MOs) does not contribute in the emission spectra. However, the charge-transfer emission band depends on the metal coordination ligand. Given the strong electron-donating ability of the thiolate ligand, it is expected that the origin of the emission is due to thiolate–copper(I) (LMCT) transition. Contributions like XMCT and XLCT may be minor, if they exist. The emission spectrum of **4** shows two bands at 436 nm and 572 nm. The low-energy emission band is attributed to thiolate–copper(I) (LMCT) transition and the high-energy band to CC origin (the Cu···Cu separation <2.8 Å). Compound **3** exhibits an emission band at 573 nm, which may originate from LMCT states in accord with the electron-donating ability of the thiolate ligands. The observed differential emission intensity must be based on the cluster size and the Cu/S stoichiometry. The loss in intensity of **1** than **2** is due to some oxidation of Cu^I to Cu^{II} during (see latter) isolation in atmospheric air. The Cu–MT proteins have been found to exhibit significant luminescence,[43–45] which is related to the Cu^I–thiolate chromophore and Cu–S protein emission lies from 580–700 nm at room temperature. Like Cu–MT proteins, clusters **1**–**4** show photoluminescence in the region around 560 nm on excitation at 350 nm (Figure 5). Interestingly, such emission property can help to identify the Cu/thiol stoichiometry in apo-NcMT proteins.[8] However, with the option of varying the ability of

complexation of Cu^I with the overall sulfahydryl groups present in such proteins, the intensity of the emission spectra may be deceptive to extract the actual stoichiometry of the Cu–MT proteins. The difference in Cu/MT stoichiometry in such reconstitution by using apo-NcMT and Zn–NcMT is noteworthy to reflect the possibility in the use of different sulfahydryl groups based on the flexibility of the MT. Complex **1** is found to be more oxygen sensitive and even in the solid its white surface slowly developed a greenish tinge and displayed the appearance of EPR-active Cu^{II} concomitant to the quenching of the emission around 560 nm (Figure 6).

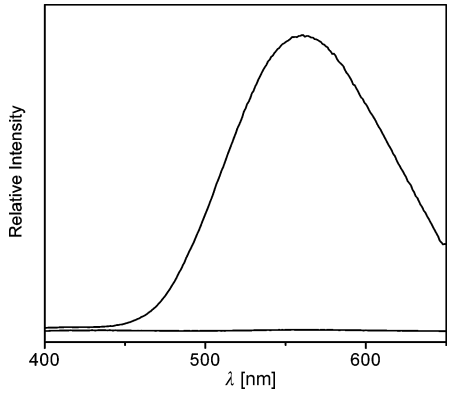

Figure 6. Emission spectra of **1** in the solid state at room temperature: (a) freshly prepared; (b) after 24 h exposure to air.

Conclusions

We demonstrated the facile interconversion of Cu–SPh clusters with different stoichiometries in relation to the flexibility of MT proteins. The structural variations in these synthesized clusters in solution clearly demonstrate their ability to shuffle copper ions interplaying the overall coordinating ability of the copper cluster, which is not dependent on the nature of the bridging thiolate ion.[46–48] It is to be noted that in the synthesized Cu_8-yeastMT cluster[10] or in Cu_7-saccharomyces cerevisiae,[12] the presence of the Cu_6 cluster is predicted because of the loose coordination of the terminal copper ions. Interestingly, the Cu–S–Cys bond (2.144 Å) between Cu44 and Cys7 is one of the shortest Cu–S–Cys bonds present in the Cu_8-yeastMT cluster,[10] but this bond is readily broken and loses the Cu44 ion in solution. This is due to the exposure of this end of the cluster to solvent where this copper can be readily dissociated in solution.[10] We also demonstrated that such copper ion shuffling is possible with a change in solvent under ambient conditions. The Cu/S ratio in Cu–MT can be affected by the surrounding environment or even be variations in the cysteine content; however, it is important to note that the availability of Cu is the key factor affecting the stoichiometry of the Cu/S clusters in MT. The well-known complexity of copper(I)–thiolates is greatly enhanced when moving towards the cysteine rich copper-metallothioneins, whose flexibility is not only due to the lability of the metal–sulfur bond but also to the mobility of the peptide chain.[10] Thus, variation in the folding in this class of proteins may be related to the uptake and release of a copper ion. The different degree of incorporation of copper ions as observed in identifying Cu_4 clusters in direct interaction with copper ions with an apo-MT is in contrast with the formation of a Cu_6 cluster formed by the displacement of a zinc ion from Zn–MT[8,49–52] and directly related to structural variations influenced by the coordination of zinc ions subsequent to their displacement by copper ions.

Experimental Section

General: All the reactions were carried out under an inert atmosphere and under ambient conditions. Et_4NBr, Et_4NCl and thiophenol were obtained from standard commercial sources. Solvents were distilled and dried by standard procedure. Elemental analyses for carbon, hydrogen, nitrogen and sulfur analysis were recorded with a Perkin–Elmer 2400 microanalyzer. Electronic spectra were recorded with a Cintra 10 UV/Vis spectrophotometer. The emission spectra were recorded with a fluorolog fluorescence spectrophotometer. EPR spectra were measured with a Varian E-109 and with a Bruker EMX X-band EPR spectrometer at room temperature in solid sample. NMR spectra were recorded with a JEOL JNM-LA 400 FT–NMR machine. $[Cu^ISPh]_n$ was prepared by a literature procedure.[33]

$[Et_4N]_4[Cu_6(SPh)_4Cl_6]$ (1): To a suspension of polymeric $[Cu^ISPh]_n$ (0.34 g, 2 mmol) in DMF (25 mL) was added Et_4NCl (0.49 g, 3 mmol). The mixture was stirred at room temperature to afford a clear-yellow solution within 10 min. An excess amount of diethyl ether (≈ 100 mL) was added to precipitate the light yellow product and this was separated by filtration, washed with 2-propanol to remove any unreacted Et_4NCl followed by diethyl ether and vacuum dried. Compound **1** was crystallized by dissolving it in DCM and by adding hexane and was isolated as colourless blocks. The crystal when free from solvent is very susceptible to loose coordinated solvent molecules, which results in opacity and brittle crystals. Freshly isolated transparent crystals on dissolution in DMSO decomposed to release Et_4NCl and the solvent in the lattice. Yield: 0.38 g (75%). ^1H NMR (400 MHz, [D$_6$]DMSO): δ = 1.154 (t, J = 7.1 Hz, 3 H, CH_3), 3.199 (q, J = 7.1 Hz, 2 H, CH_2), 5.731 (s, 2 H) ppm. NMR showed the presence of CH_2Cl_2; proton integration provided roughly $1.5CH_2Cl_2$ per molecule of the complex. $C_{56}H_{100}Cl_6Cu_6N_4S_4$ (1551.69): calcd. C 43.31, H 6.44, N 3.61, S 8.25; found C 43.45, H 6.62, N 3.57, S 8.23.

$[Et_4N]_4[Cu_6(SPh)_4Br_6]$ (2)

Method 1: A procedure similar to that described for the synthesis of **1** was carried out with Et_4NBr (0.66 g, 3 mmol) in place of Et_4NCl to afford a light yellow precipitate. Compound **2** crystallized from DCM/hexane as colourless blocks. Yield: 0.48 g (80%).

Method 2: To a solution of **3** (0.34 g, 0.25 mmol) in DMF (25 mL) was added an excess amount of Et_4NBr. The mixture was stirred to afford a light yellow solution within 15 min. An excess amount of diethyl ether (≈ 100 mL) was added to precipitate the crude product. This was separated by filtration and washed with 2-propanol to free it from excess Et_4NBr. The product was crystallized from DCM/hexane as colourless blocks. The ready loss of solvent for this complex is similar to that observed with **1**. Yield: 0.31 g (65%). ^1H NMR (400 MHz, [D$_6$]DMSO): δ = 1.145 (t, J = 7.1 Hz, 3 H, CH_3), 3.192 (q, J = 7.1 Hz, 2 H, CH_2), 5.734 (s, 2 H) ppm. NMR showed the presence of CH_2Cl_2 and integration provided $1.5CH_2Cl_2$ per molecule of **2**. $C_{56}H_{100}Br_6Cu_6N_4S_4$ (1818.38): calcd. C 36.96, H 5.5, N 3.08, S 7.04; found C 37.02, H 5.68, N 2.99, S 7.01.

$[Et_4N]_2[Cu_5(SPh)_7]$ (3)

Method 1: To a solution of **2** (0.45 g, 0.25 mmol) in DCM (25 mL) was added a mixture of HSPh (1 mL) and Et_3N (0.5 mL). The mixture was stirred at room temperature to afford a light-yellow solution. Into this solution was added hexane (15 mL) and on standing overnight at 0 °C bright-yellow crystals had separated out. These were separated by filtration, washed with hexane and dried in vacuo. Yield: 0.27 g (68%).

Method 2: To a suspension of $[Cu^{I}SPh]_n$ (0.34 g, 2 mmol) in DMF (25 mL) was added Et_4NCl (0.49 g, 3 mmol). The mixture was stirred at room temperature to afford a clear-yellow solution. Into this solution was added diethyl ether (≈15 mL) and on standing at 0 °C overnight bright-yellow crystals had separated out. Product **3** was separated by filtration, washed with 2-propanol, ether and dried in vacuo. Yield: 0.23 g (62%). $C_{58}H_{75}Cu_5N_2S_7$ (1342.44): calcd. C 51.85, H 5.59, N 2.09, S 16.69; found C 51.82, H 5.57, N 2.06, S 16.66.

$[Et_4N]_2[Cu_4(SPh)_6]\cdot 0.5C_3H_8O$ (4): To a solution of **2** (0.45 g, 0.25 mmol) in DMF (25 mL) was added a mixture of HSPh (1 mL) and Et_3N (0.5 mL). The mixture was stirred for 15 min at room temperature to afford a light-yellow solution. Into this solution was added 2-propanol (40 mL) and on standing at 0 °C overnight pale-yellow crystals had separated out. The crystals were separated by filtration, washed with diethyl ether and dried in vacuo. Yield: 0.30 g (70%). ^{1}H NMR (400 MHz, [D$_6$]DMSO): δ = 1.068 (t, J = 5.6 Hz, 3 H, CH_3), 3.095 (q, J = 7.1 Hz, 2 H, CH_2), 6.7498 (m, 2 H, *p*-Ph), 7.316 (d, J = 6.9 Hz, 2 H, *o*-Ph) ppm. ^{13}C NMR (100 MHz, [D$_6$]-DMSO): δ = 7.011 (-CH_3), 25.440 (α-C of *i*PrOH), 51.429 (-CH_2-), 121.203 (*p*-Ph), 126.781 (*m*-Ph), 132.557 (*o*-Ph), 145.449 (1C-Ph) ppm. On the basis of the integration of the protons from the phenyl and alkyl groups of the main complex, the extra alkyl protons found were assigned to the *i*PrOH molecules present in the lattice. $C_{53.5}H_{74}Cu_4N_2O_{0.5}S_6$ (1199.72): calcd. C 53.51, H 6.17, N 2.33, S 16.00; found C 53.48, H 6.12, N 2.36, S 16.09.

X-ray Crystallography: Suitable diffraction quality crystals were obtained from the crystallization procedures described in each synthesis. The crystals used in the analyses were glued to a glass fibre and mounted on a BRUKER SMART APEX diffractometer. The instrument was equipped with CCD area detector and data were collected by using graphite-monochromated Mo-K_α radiation (λ = 0.71069 Å) at low temperature (100 K). All empirical absorption corrections were applied by using the SADABS program. Cell constants were obtained from the least-squares refinement of three-dimensional centroids through the use of CCD recording of narrow ω rotation frames, completing almost all-reciprocal space in the stated θ range. All data were collected with SMART 5.628 (BRUKER, 2003), and were integrated with the BRUKER SAINT program. The structure was solved by using SIR97 and refined with the use of SHELXL-97.[53] The space group of those compounds was determined on the basis of the lack of systematic absence and intensity statistics. Full-matrix least-squares/difference Fourier cycles were performed which located the remaining non-hydrogen atoms. All non-hydrogen atoms were refined with anisotropic displacement parameters. Each complex (**1**, **2** and **3**) possesses only one molecule in their respective asymmetric unit. In the asymmetric unit of compound **4**, there are two independent Cu_4 units. The additional symmetry for **4** was checked through PLATON.[54,55] Single crystals of complex **4** were grown from three different batches but all these possess similar crystallographic asymmetric unit. Some of the carbon atoms of ethyl groups of tetraethylammonium cation were disordered for **1**, **2**, **3** and **4** and refined with free part instruction by using SHELXL-97. The structures of **1**, **2** and **4** suffered from disordered and unidentified solvent (DCM/Hexane for **1**, **2** and 2-propanol for **4**) in the lattice, which was not included in the refinement but was taken care of by the SQUEEZE-procedure (from PLATON).[54,55] The volumes occupied by the solvent were 1049.5, 1115.6 and 214.4 Å^3, respectively; the numbers of electrons per unit cell deduced by SQUEEZE were 139, 146 and 26. All hydrogen atoms were placed in idealized calculated positions and allowed to ride on their corresponding carbon atoms with fixed isotropic contributions. Further information on crystal data, data collection and structure refinement are summarized in Table 3. Disordered solvent molecule of **1** and **2** were squeezed by using PLATON and details of squeeze results were appended to the crystallographic data file. CCDC-616824 to -616827 contain the supplementary crystallographic data for this paper. These data can be obtained free of charge from The Cambridge Crystallographic Data Centre via www.ccdc.cam.ac.uk/data_request/cif.

Supporting Information (see footnote on the first page of this article): UV/Vis and NMR spectra of synthesized complexes.

Table 3. Crystallographic data[a] and refinement details for complexes of **1**, **2**, **3** and **4**.

Complexes	**1**	**2**	**3**	**4**
Formula	$C_{56}H_{100}Cl_6Cu_6N_4S_4$	$C_{56}H_{100}Br_6Cu_6N_4S_4$	$C_{58}H_{75}Cu_5N_2S_7$	$C_{52}H_{70}Cu_4N_2S_6$
Formula weight	1551.69	1818.38	1342.44	1169.72
Crystal system	triclinic	triclinic	triclinic	triclinic
Space group	$P\bar{1}$	$P\bar{1}$	$P\bar{1}$	$P\bar{1}$
T [K]	100(2)	100(2)	100(2)	100(2)
Z	2	2	2	4
a [Å]	13.77(5)	14.145(5)	12.374(5)	17.072(5)
b [Å]	18.100(5)	18.065(5)	13.047(5)	18.633(5)
c [Å]	18.109(5)	18.333(5)	20.828(5)	18.648(5)
α [°]	100.936(5)	100.416(5)	93.545(5)	109.482(5)
β [°]	107.023(5)	107.354(5)	106.841(5)	91.779(5)
γ [°]	95.100(5)	95.409(5)	112.367(5)	93.123(5)
V [Å^3]	4186(2)	4343(2)	2919.4(18)	5576(3)
$D_{calcd.}$ [g cm^{-3}]	1.231	1.390	1.527	1.393
μ [mm^{-1}]	1.818	4.328	2.081	1.764
θ range [°]	2.00–28.30	2.07–28.35	2.07–28.35	2.17–28.33
GOF (F_2)	1.117	0.939	1.091	1.119
R_1[b]	0.0659	0.070	0.0727	0.0711
wR_2[c]	0.1496	0.1692	0.1474	0.1419

[a] Mo-K_α radiation. [b] $R_1 = \sum||F_o| - |F_c||/\sum|F_o|$. [c] $wR_2 = \{\sum[w(F_o^2 - F_c^2)^2]/\sum[w(F_o^2)^2]\}^{1/2}$.

Acknowledgments

B. K. M. and K. P. gratefully acknowledge doctoral fellowships from the UGC and the CSIR, New Delhi, respectively; S. S. thanks DST, New Delhi for funding.

[1] J. D. Otvos, I. M. Armitage, *Proc. Natl. Acad. Sci. USA* **1980**, *77*, 7094.
[2] D. R. Winge, K. A. Miklossy, *J. Biol. Chem.* **1982**, *257*, 3471.
[3] K. B. Nielson, D. R. Winge, *J. Biol. Chem.* **1984**, *259*, 4941.
[4] M. J. Stillman, A. J. C. Law, W. Cai, A. J. Zelazowski, *Experientia Suppl.* **1987**, *52*, 203.
[5] J. H. R. Kägi, Y. Kojima, *Experientia Suppl.* **1987**, *52*, 25.
[6] Y. J. Li, U. Weser, *Inorg. Chem.* **1992**, *31*, 5526.
[7] M. J. Stillman, *Coord. Chem. Rev.* **1995**, *144*, 461A.
[8] P. A. Cobine, R. T. McKay, K. Zangger, C. T. Dameron, I. M. Armitage, *Eur. J. Biochem.* **2004**, *271*, 4213.
[9] B. Roschitzki, M. Vašák, *J. Biol. Inorg. Chem.* **2002**, *7*, 611.
[10] V. Calderone, B. Dolderer, H. J. Hartmann, H. Echner, C. Luchinat, C. D. Bianco, S. Mangani, U. Weser, *Proc. Natl. Acad. Sci. USA* **2005**, *102*, 51.
[11] H. J. Hartmann, U. Weser, *Biochim. Biophys. Acta* **1988**, *953*, 1.
[12] Z. Xiao, F. Loughlin, G. N. George, G. J. Howlett, A. G. Wedd, *J. Am. Chem. Soc.* **2004**, *126*, 3081.
[13] I. Bertini1, H. Hartmann, T. Klein, G. Liu1, C. Luchinat, U. Weser, *Eur. J. Biochem.* **2000**, *267*, 1008.
[14] I. G. Dance, *Polyhedron* **1986**, *5*, 1037.
[15] P. J. Blower, J. R. Dilworth, *Coord. Chem. Rev.* **1987**, *76*, 121.
[16] G. Henkel, B. Krebs, *Chem. Rev.* **2004**, *104*, 801.
[17] K. Fujisawa, S. Imai, N. Kitajima, Y. Moro-oka, *Inorg. Chem.* **1998**, *37*, 168.
[18] D. Coucouvanis, C. N. Murphy, S. K. Kanodia, *Inorg. Chem.* **1980**, *19*, 2993.
[19] C. D. Garner, J. R. Nicholson, W. Clegg, *Inorg. Chem.* **1984**, *23*, 2148.
[20] R. K. Chadha, R. Kumar, D. G. Tuck, *Can. J. Chem.* **1987**, *65*, 1336.
[21] I. G. Dance, L. J. Fitzpatrick, M. L. Scudder, *J. Chem. Soc. Chem. Commun.* **1983**, 546.
[22] E. Block, H. Kang, G. Ofori-Okai, J. Zubieta, *Inorg. Chim. Acta* **1990**, *167*, 147.
[23] M. Baumgartner, W. Bencsh, P. Hug, E. Dubler, *Inorg. Chim. Acta* **1987**, *136*, 139.
[24] J. R. Nicholson, I. L. Abrahams, W. Clegg, C. D. Garner, *Inorg. Chem.* **1985**, *24*, 1092.
[25] I. G. Dance, J. C. Calabrese, *Inorg. Chim. Acta* **1976**, *19*, L41.
[26] G. A. Bowmaker, G. R. Clark, I. G. Dance, *Polyhedron* **1983**, *2*, 1031.
[27] G. A. Bowmaker, G. R. Clark, J. K. Seadon, I. G. Dance, *Polyhedron* **1984**, *3*, 535.
[28] I. G. Dance, *J. Chem. Soc. Chem. Commun.* **1976**, 68.
[29] I. G. Dance, *Aust. J. Chem.* **1978**, *31*, 2195.
[30] M. Baumgartner, H. Schmalle, E. Dubler, *Polyhedron* **1990**, *9*, 1155.
[31] I. Schroeter-Schmid, J. Z. Straehle, *Z. Naturforsch., Teil B* **1990**, *45*, 1537.
[32] E. Block, M. Gernon, H. Kang, G. Ofori-Okai, J. Zubieta, *Inorg. Chem.* **1989**, *28*, 1263.
[33] I. G. Dance, P. J. Guerney, A. D. Rae, M. L. Scudder, *Inorg. Chem.* **1983**, *22*, 2883.
[34] The syntheses of **3** and **4** were earlier reported by different methods, but mixtures of both **3** and **4** or poor diffraction-quality crystals were obtained. See refs.[18,23–26,29]
[35] B. L. Hathaway, *Comprehensive Coordination Chemistry* (Ed.: G. Wilkinson), Pergamon, Oxford, England, **1987**, vol. 5, p. 533.
[36] I. G. Dance, *J. Chem. Soc. Chem. Commun.* **1976**, 68.
[37] Compounds **1**, **2** in this work.
[38] B. K. Maiti, K. Pal, S. Sarkar, *Inorg. Chem. Commun.* **2004**, *7*, 1027.
[39] A. N. M. Lanfredi, A. Tiripicchio, A. Camus, N. Marsich, *J. Chem. Soc. Dalton Trans.* **1989**, 753.
[40] R. V. Parish, Z. Salehi, R. G. Pritchard, *Angew. Chem. Int. Ed. Engl.* **1997**, *36*, 251.
[41] P. C. Ford, E. Cariati, J. Bourassa, *Chem. Rev.* **1999**, *99*, 3625.
[42] V. W. W. Yam, K. K. W. Lo, *Chem. Soc. Rev.* **1999**, *28*, 323.
[43] A. R. Green, M. J. Stillman, *Inorg. Chim. Acta* **1994**, *226*, 275.
[44] M. Beltramini, K. Lerch, *FEBS Lett.* **1981**, *127*, 201.
[45] G. Meloni, P. Faller, M. Vasák, *J. Biol. Chem.* **2007**, *282*, 16068.
[46] I. J. Pickering, G. N. George, C. T. Dameron, B. Kurz, D. R. Winge, I. G. Dance, *J. Am. Chem. Soc.* **1993**, *115*, 9498.
[47] T. A. Smith, K. Lerch, K. O. Hodgson, *Inorg. Chem.* **1986**, *25*, 4611.
[48] G. N. George, J. Byrd, D. R. Winge, *J. Biol. Chem.* **1988**, *263*, 8199.
[49] M. Beltramini, K. Lerch, *Biochemistry* **1983**, *22*, 2043.
[50] M. Beltramini, G. M. Giacometti, B. Salvato, G. Giacometti, K. Muenger, K. Lerch, *Biochem. J.* **1989**, *260*, 189.
[51] A. R. Green, A. Presta, Z. Gasyna, M. J. Stillman, *Inorg. Chem.* **1994**, *33*, 4159.
[52] K. Fujisawa, S. Imai, S. Suzuki, Y. Moro-oka, Y. Miyashita, Y. Yamada, K. Okamoto, *J. Inorg. Biochemistry* **2000**, *82*, 229.
[53] G. M. Sheldrick, *SHELXL-97: Program for Crystal Structure Refinement*, University of Göttingen, Germany, **1997**.
[54] A. L. Spek, *PLATON*, University of Utrecht, The Netherlands, **2001**.
[55] A. L. Spek, *Acta Crystallogr., Sect. A* **1990**, *46*, 194.

Received: July 24, 2007
Published Online: October 25, 2007

